DOI: 10.1002/ejic.200801194

"One-Pot" Ion-Exchange and Mesopore Formation During Desilication

Martin Spangsberg Holm,*[a,b] Martin Kalmar Hansen,[a] and Claus Hviid Christensen*[b]

Keywords: Zeolites / Mesoporous materials / Desilication / Ion exchange

A desilication protocol using tetramethylammonium hydroxide was applied to zeolite beta. The new route presented here integrates the desilication and ion-exchange post-treatment steps allowing for a subsequent ion-exchange step to be avoided. It is shown that the acidic and highly mesoporous zeolite is obtained directly upon calcination. Thus, careful choice of base and post-treatment conditions lead to the fabrication of a hierarchical *meso*- and microporous structure with completely retained crystallinity.

(© Wiley-VCH Verlag GmbH & Co. KGaA, 69451 Weinheim, Germany, 2009)

Introduction

Zeolites are microporous crystalline materials composed of tetrahedral oxides of silicon and aluminum. The framework is formed through corner sharing of the oxygen atoms giving rise to a multitude of structures.[1] The micropore diameters of the zeolite structures are in the range of small organic molecules, which cause the molecular sieves ability and allow for shape selective catalysis. Slow molecular transport through the microporous channels may however limit the applicability of zeolites as catalysts.[2] Various strategies for introducing mesoporosity are now available to overcome this limitation by producing hierarchical zeolite materials.[3] Well known protocols include dealumination,[4] templating[5] and desilication.[6] Recently, several studies in which desilication is applied to the widely used high-silica zeolite ZSM-5 have been published.[7] Additional zeolite structures e.g. beta,[8] ZSM-12[9] and mordenite[10] have also been investigated. Sodium hydroxide and/or sodium carbonate[11] are the typical bases applied, although lithium hydroxide and potassium hydroxide have proven useful as well.[12] Adjustment of temperature, amount of base, and duration of the treatment are effective tools for controlling the extent of mesopore formation. However, even surprisingly mild conditions applied in attempts to desilicate zeolite beta with a mineral base were unable to create mesoporosity without seriously deteriorating the crystal structure.[8] In addition, use of mineral bases causes ion-exchange of the zeolite into the alkali form. This highlights two inherent shortcomings of the use of strong inorganic bases in the desilication protocol.Here, we use tetramethylammonium hydroxide (TMAOH in the following) as the desilicating agent, and show that it leads to several interesting advantages. A "one-pot" desilication and ion-exchange procedure as reported here gives a procedure in which a subsequent ion-exchange step transforming the zeolite into proton form is avoided. This is possible since the charge compensating TMA^+ ions in the zeolite framework decomposes during calcination to give the proton form. TMAOH was specifically chosen as the organic base due to its inherent strong basicity and the relative small size of the TMA^+ cation. Mesopore formation using TMAOH was studied as a function of treatment time, temperature, and base amount. The extent of the simultaneous ion-exchange was monitored by NH_3-TPD and FT-IR.

[a] Center for Sustainable and Green Chemistry, Department of Chemistry, Technical University of Denmark, Building 206, 2800 Lyngby, Denmark
[b] Haldor Topsoe A/S, Nymøllevej 55, 2800 Lyngby, Denmark
E-mail: chc@topsoe.dk

Results and Discussion

A zeolite beta was synthesized by the fluoride route with a nominal Si/Al ratio of 35. This aluminum content has previously been identified as within the optimal range for desilication of ZSM-5.[13] The crystalline zeolite beta was initially ion-exchanged into the sodium form to allow the transformation from Na-form into H-form to occur during post-treatment. The series of desilications were performed according to the conditions listed in Table 1. The desilication conditions were chosen to investigate the effect on mesopore formation arising from temperature, time and TMAOH amount present.

Figure 1 presents the XRPD diffractograms of the parent sample along with the most severely desilicated samples chosen from Table 1. The parent sample is identified as highly crystalline zeolite beta which is also supported by a t-plot derived micropore volume of 0.202. Further it is seen from Figure 1, that all samples desilicated using TMAOH (samples 4, 7, 11) preserve crystallinity. A mild treatment using NaOH as the desilication agent instead of TMAOH was included for comparison (sample 12). In contrast to samples 1–11, sample 12 has lost almost all crystallinity as

 WILEY InterScience DISCOVER SOMETHING GREAT © 2009 Wiley-VCH Verlag GmbH & Co. KGaA, Weinheim

Table 1. Treatment conditions and physical-chemical data.

Sample	TMA media [mmol/g]	Time [h]	Temp. [°C]	TMA^+/Na^+ ratio[a]	S_{BET} [m^2/g]	S_{meso} [m^2/g]	V_{meso} [mL/g] ($P_{0.99} - V_{micro}$)	V_{micro} [mL/g]	Acidity[b] [mmol/g]	Exchange level[c]
Parent	–	–	–	–	539	66	–	0.202	0.21	–
1	10	1/2	65	20	551	93	≈ 0	0.205	0.21	0.82
2	10	2	65	20	561	114	0.076	0.198	0.24	0.91
3	10	4	65	20	585	125	0.150	0.201	0.24	1.00
4	10	6	65	20	599	140	0.173	0.197	0.24	1.02
5	10	2	50	20	531	95	≈ 0	0.194	0.22	0.82
6	10	2	80	20	601	141	0.193	0.196	0.24	1.07
7	10	2	100	20	696	266	0.364	0.186	0.28	1.10
8	2.5	2	65	5	540	106	0.034	0.193	0.23	0.97
9	5	2	65	10	563	118	0.084	0.197	0.23	1.04
10	20	2	65	40	560	107	0.083	0.200	0.24	0.86
11	50	2	65	100	559	106	0.045	0.203	0.23	0.71
12	10 (NaOH)	1/2	65	–	787	489	0.304	0.081	–	–

[a] Approximate value assuming one sodium ion per Al atom and a zeolite with Si/Al ratio of 35. [b] NH_3-TPD of the ion-exchanged material. [c] Ratio between the integrated area of the NH_3-desorption curve before and after ion-exchange.

seen from Figure 1, which is also indicated by a diminished micropore volume of only 0.081 mL/g. This is in agreement with results published recently on desilication of zeolite beta using NaOH.[8] The mesopore formation using TMAOH progresses slower than what is typically observed for desilication using NaOH.[8,14] Extending treatment time from 1/2 hour to as much as 6 h allows for continuous mesopore evolution as can be seen from the textural data in Table 1 (samples 1–4). A gradual increase in the mesopore volume V_{meso} and the mesopore surface area S_{meso} are thus observed as a function of treatment time. Isotherms and the BJH-derived pore size distributions for samples parent, 1–4, and 12 are given in Figure 2. Sorption data from sample 12 which was desilicated by NaOH are included in Figure 2. The isotherms from sample 12 do neither resemble a type I isotherm as is typical seen for a microporous materials nor one for a combined micro- and mesoporous material as can be seen for the TMAOH-desilicated samples. This observation correlates well with the results obtained from XRD analysis indicating that a partial framework collapse occur when using NaOH but can be avoided by using TMAOH.

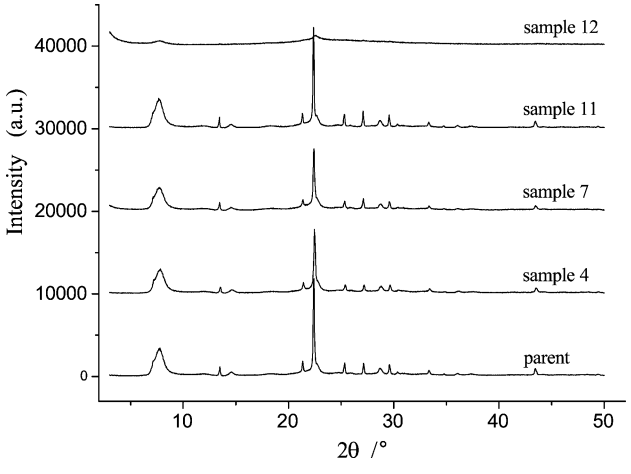

Figure 1. XRPD diffractograms of selected samples from Table 1. Diffractograms are offset by 10000 units for illustrative purposes.

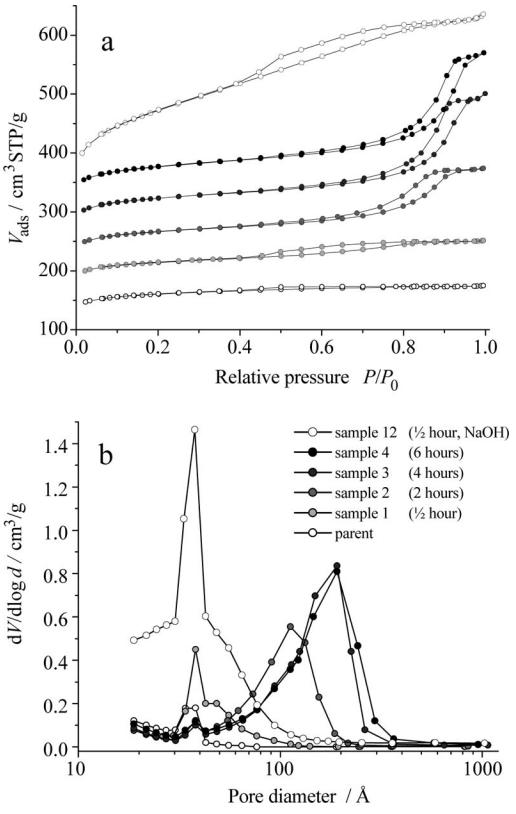

Figure 2. (a) N_2-adsorption/desorption isotherms of samples 1–4 and 12. Isotherms are offset by 50 units for illustrative purposes. (b) BJH-derived pore size distributions.

The important experimental parameters with respect to mesopore generation was systematically investigated by varying the temperature in samples 5–7 and the amount of TMAOH in samples 8–11. Interestingly, as the temperature is increased from 50 °C to 100 °C, the mesopore formation accelerates as illustrated by the isotherms in Figure 3 (a). The BJH-derived pore size distributions are shown in part b of Figure 3. From Figure 3 (b) it can be seen that pores are gradually forming within the mesopore range (2–50 nm)

 © 2009 Wiley-VCH Verlag GmbH & Co. KGaA, Weinheim

and that the pore diameter increases as a function of temperature. The mesopore volume clearly increases in a similar way to as much as 0.364 mL/g for sample 7. Further analyzing the sorption data, it is interesting to note that at prolonged desilication times and at high temperatures, we observe a slight decrease in the micropore volume of up to ca. 8% (sample 7, desilicated at 100 °C), which indicate that crystallinity of these samples may be slightly reduced. This is in line with expectation since previous studies have reported similar observations on mesoporous structures.[15] Samples 2, 8–11 highlight the effect on mesoporosity when increasing the amount of TMAOH. This post-treatment parameter is very important in this new desilication protocol since we aim to quantitatively exchange Na^+ as the charge compensating cation with TMA^+ during the treatment. Sodium is present as the charge compensation cation in the starting material. In Table 1 it is shown that a TMAOH amount of 10 mmol/g leads to an approximate TMA^+/Na^+ ratio of 20. This ratio is estimated from the theoretical aluminum density in a framework with an Si/Al ratio of 35 and assuming complete initial charge compensation by sodium. Varying the TMAOH amount between 5 and 20 mmol/g during desilication (samples 2, 9, and 10) lead only to minor variations in the mesopore formation. However, a decrease and surprisingly also an increase by a factor of 4 (samples 8, and 11) both lead to a limited mesopore formation. The modest mesoporosity formed when as much as 50 mmol/g TMAOH was used could be explained by a structure stabilizing ability of the TMA^+ ion, since it resembles the template (TEA^+) typically used in the synthesis crystallizing zeolite beta.

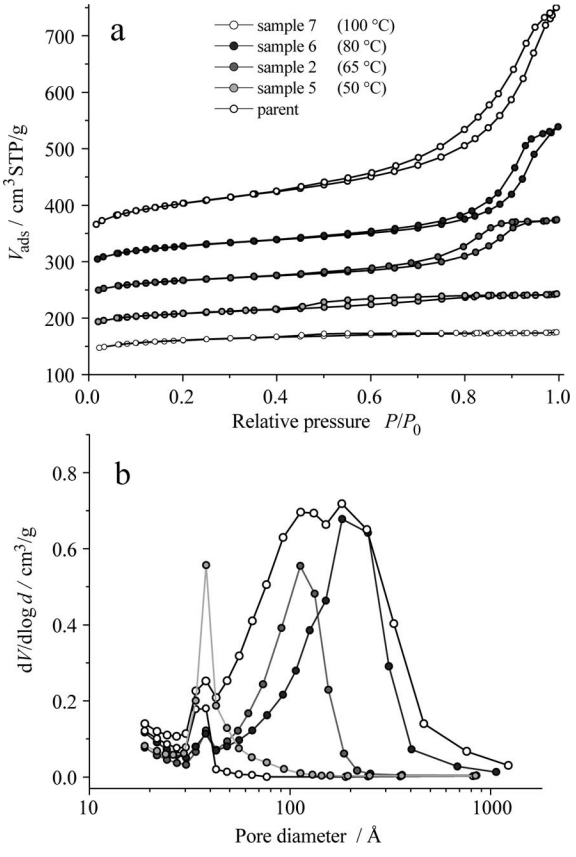

Figure 3. N_2-adsorption/desorption isotherms. (a) Increasing treatment temperature. (b) BJH-derived pore size distributions. Isotherms in (a) are offset by 50 units in relation to the previous for illustrative purposes.

NH_3-TPD was used to monitor the acidity of the zeolites. The acidity of the desilicated samples 1–11 were measured after calcination at 550 °C for 6 h in static air. Following this measurement the samples were ion-exchanged completely into H-form and the acidity measurements by NH_3-TPD were repeated. By comparing the two values, before and after ion-exchange, we were able to monitor whether the TMAOH desilication followed by calcination directly produced the protonic form of the zeolite. Figure 4 shows the NH_3-TPD curves of sample 2 before and after ion-exchange. We observe two very similar ammonia desorptions profiles both with a maximum around 345 °C corresponding to ammonia desorbing from the strong Brønsted acidic bridging hydroxy group. The integrated area under the curve corresponds to a measure of the total acidity. A slight increased is apparent after the ion-exchange in the case of sample 2. We interpreted this as the majority of the treated zeolite being transferred into proton form directly by the TMAOH desilication. However, the difference between the curves ist likely due to minor amounts of sodium still performing the charge compensation. The ratio between the integrated area of the two NH_3-desorption curves is thus a measure of the level of ion-exchange obtained directly from the TMAOH desilication. This ratio for all samples is listed in Table 1. For the most interesting samples, we observe very high exchange levels close to unity. This means that it is possible to obtain close to complete ion-exchange by combining the desilication and calcination procedures. Surprisingly, some of the most harshly desilicated samples (samples 6, 7 and 9) show an exchange level slightly above 1. This could be explained by the formation of extra framework aluminum (EFAL) as a consequence of harsh desilication which would introduce Lewis acidity.[16] Possibly

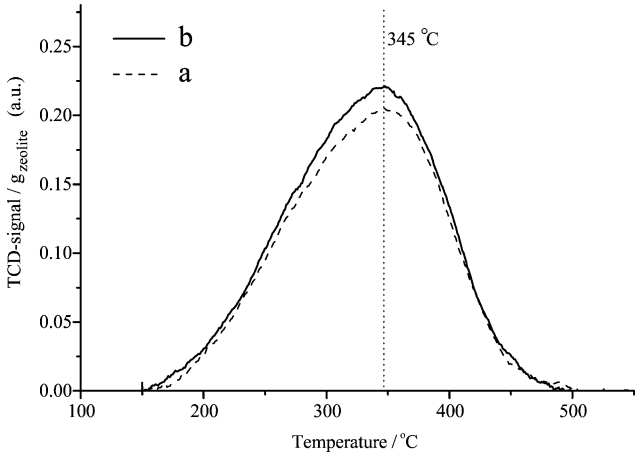

Figure 4. NH_3-TPD of (a) sample 2 after TMAOH desilication and calcination and (b) sample 2 ion-exchanged into proton form.

 © 2009 Wiley-VCH Verlag GmbH & Co. KGaA, Weinheim

these extra framework aluminum species could solely contribute to the acidity before the ion-exchange due to removal during the ion-exchange procedure. Importantly, it is seen that increasing the TMAOH amount above 5 mmol/g decreases not only the mesopore surface area S_{meso} but also the level of ion-exchange obtained. This shows that huge amounts of TMAOH is not necessarily required to obtain a quantitatively ion-exchange into the proton form. We hypothesize that the ion-exchange is positively affected by a high affinity of sodium to coordinate to dissolved silicate species compared to performing the charge compensation. Further in Table 1, it is summarized that in all cases where mesoporosity is formed, an increase in total acidity is seen. This is in line with expectations from the selective silicon extraction.[14]

NH_3-TPD does not discriminate between Lewis and Brønsted acidity. However, a IR absorption at ca. 3610 cm^{-1} in the zeolite originates from the Brønsted acidic bridging hydroxy group.[17] Figure 5 presents the FT-IR absorption spectra of the parent sample in sodium and protonic form along with sample 3 which was desilicated with TMAOH and subsequently calcined. From Figure 5 it is seen that the 3610 cm^{-1} band is absent in the sodium form (a) but clearly present in the protonic form (b) of the parent sample. After the desilication process the band at 3610 cm^{-1} is reintroduced in spectrum (c) confirming that the treated zeolite indeed contains conventional Brønsted acidic sites. This information supports the previous observations that it is possible to perform the ion-exchange and mesopore formation in one synthesis step.

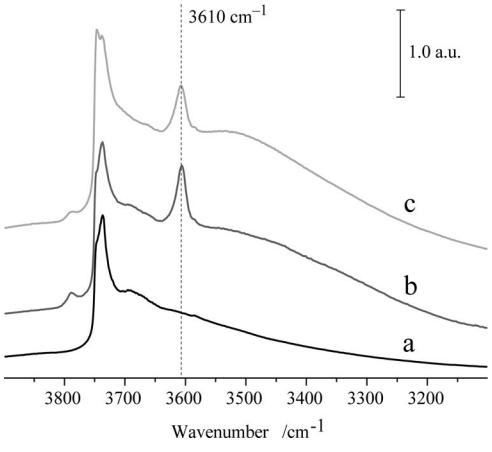

Figure 5. FT-IR absorption spectra of (a) parent sample in sodium form, (b) parent sample in protonic form and (c) sample 3 (TMAOH-desilicated and calcined). Spectra normalized to the framework overtones and offset for illustrative reasons.

Scanning electron microscopy was applied to study morphology changes in the material. For the parent zeolite a narrow crystal size distribution centered on 10 μm are found as can be seen in Figure 6A. Image 6B (sample 3) is an example of how the crystals can be partly deteriorated mainly at the top and bottom of the bipyramidal structure as a function of the desilication.

Image 6C and 6D (samples 6 and 7) reveal how increased temperature during treatment affects the crystals. Image 6C

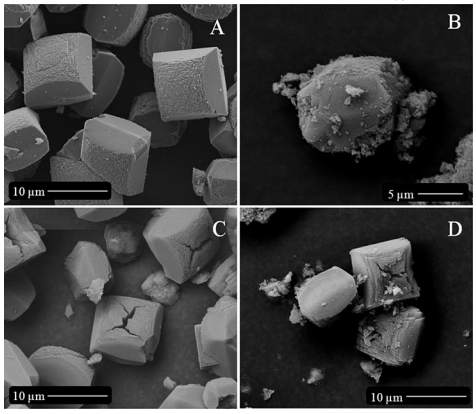

Figure 6. SEM images of the parent sample (a), sample 3 (b), sample 6 (c) and sample 7 (d).

show the presence of large cracks in the crystals. A further temperature increase to 100 °C in 6D leads to a similar behavior but additionally tends to create more crystal debris and partly destroy the original crystal morphology. It is, however, unlikely that the crystal debris is amorphous material since we observe essentially no changes in the diffractograms of these samples and only a minor decrease in micropore volume. Since we are able to introduce mesoporosity as seen in 6C before we observe substantial crystal dismantling, we interpret the micrographs as it is possible to create intra rystal mesoporosity by desilicating with TMAOH. Contributions to the overall porosity from intercrystal voids could though be substantial in cases of severe desilication conditions. Interestingly, desilicating zeolite beta initially in protonic form, i.e. without sodium present using TMAOH results only in limited mesopore formation. In this case we know that one equivalent of base is consumed to neutralize the solid acid and TMA^+ is localized near the aluminum to charge compensate the framework. However, the results obtained from varying the base amounts indicate that a slight decrease in total OH^- in the solution is unlikely to be the sole explanation for a different degree of mesopore formation. Rather this result indicates that Na^+ is needed for the hydrolysis of the Si–O–Si bond to proceed effectively, somewhat similar to the mineralizing ability during synthesis. One should note the close resemblance between typical synthesis conditions and the desilication conditions used in this study. That is a highly basic aqueous suspension of the zeolite with a tetraalkylammonium cation present. Based on this, we hypothesize that the TMA^+ ion is able to stabilize the zeolite structure during desilication. This could explain why the structure does not collapse as was seen when using NaOH.[8] Potentially also important is the fact that without sodium present during the desilication the framework will be charge compensated solely by the bulky TMA^+ ion which could increase diffusion restraints and thereby prevent or simply slow the pore formation. Considering we are trying to desilicate a structure containing a relative high amount of aluminum (Si/Al: 35) this could very well be a limiting factor.

 © 2009 Wiley-VCH Verlag GmbH & Co. KGaA, Weinheim

Conclusions

In conclusion we have demonstrated how a tetraalkylammonium base is useful for desilication of zeolite beta. The procedure combines the desilication and ion-exchange steps in the direct preparation of a highly mesoporous and acidic zeolite. Further, mesopore sizes and volumes may to some extend be controlled, though not totally independent from each other. The presented study highlights the importance of proper base choice when introducing mesoporosity into zeolite structures by desilication. It shows that for specific zeolite structures, it is necessary to carefully search for the optimal base that stabilize the zeolite structure during desilication. This approach is expected to be useful for achieving hierarchical forms of other zeolites by the desilication protocol.

Experimental Section

General: Zeolite beta with a nominal Si/Al ratio of 35 was synthesized by the fluoride route using a slightly modified procedure published elsewhere.[18]

Preparation of the Synthesis Gel: Solid aluminum was dissolved in an aqueous solution (40 wt.-%) of tetraethylammonium hydroxide. After approximately one hour, a clear solution was obtained, and TEOS was slowly added over 30 min. The mixture was left for ca. 20 h with stirring at room temp. to hydrolyze TEOS and promote evaporation of ethanol, along with some water, producing a highly viscous gel. HF (40 wt.-%) was subsequently added dropwise with rapid stirring. The resulting white rigid gel with a molar oxide composition: 1 SiO_2/0.0143 Al_2O_3/0.275 $(TEA)_2O$/0.55 F was transferred to a Teflon® cup and crystallized under static conditions in a sealed stainless steel autoclave kept at 140 °C for 7 d. The crystalline zeolite was isolated by suction filtration and washed twice by re-dispersion in demineralized water. The organic template was removed by calcination at 550 °C in static air for 12 h using a heating ramp of 2 °C/min.

Typical Desilication: The zeolite (in sodium form) was suspended in hot 0.1 M aqueous TMAOH. The reaction was stopped by cooling the container in an ice bath and subsequently isolating the zeolite by suction filtration. The zeolite was washed thoroughly in demineralised water, dried at 110 °C overnight and calcined in static air at 550 °C for 6 h using a heating ramp of 2 °C/min. This calcined sample is denoted "before ion-exchange" in the text above. The proton or sodium form of the zeolite was obtained by threefold ion-exchange in a 1 M NH_4NO_3 or 1 M NaCl solution, respectively followed by calcination at 550 °C for 6 h. The proton form obtained this way is denoted "after ion-exchange" in the text above.

The samples were characterized by XRPD, N_2-sorption, FT-IR, NH_3-TPD and SEM. XRPD analysis were performed on a Bruker AXS powder diffractometer. N_2-sorption experiments were done using a Micromeritics ASAP 2020 apparatus. Prior to N_2-sorption the samples were outgassed in vacuo at 200 °C for 4 h. For FT-IR the zeolites were pressed into self supporting wafers and dehydrated at 400 °C for 2 h prior to analysis. A BioRad FTS 80 spectrometer equipped with a MCT detector was used. A Micromeretics Autochem II equipped with a TCD detector was used for NH_3-TPD experiments. Dry weights of the samples were obtained after outgassing in vacuo at 300 °C for 1 h. The NH_3 desorption curve was measured after desorption of physi-sorbed ammonia for 4 h at a temperature of 150 °C while kept in a He flow of 25 mL/ min. SEM images of the platinum/palladium-coated samples were obtained with a Philips XL 30 ESEM-FEG equipment.

Acknowledgments

The Center for Sustainable and Green Chemistry is sponsored by the Danish National Research Foundation. The authors thank Bodil F. Holten and Sven Ullmann for technical assistance.

[1] www.iza-structure.org/databases (accessed December **2008**).
[2] a) Y. Tao, H. Kanoh, L. Abrams, K. Kaneko, *Chem. Rev.* **2006**, *106*, 896; b) A. Corma, *Chem. Rev.* **1997**, *97*, 2373.
[3] J. Cejka, S. Mintova, *Catal. Rev.* **2007**, *49*, 457.
[4] A. H. Janssen, A. J. Koster, K. P. Jong, *J. Phys. Chem. B* **2002**, *106*, 11905.
[5] a) H. Wang, T. J. Pinnavaia, *Angew. Chem. Int. Ed.* **2006**, *118*, 7765; b) C. J. H. Jacobsen, C. Madsen, J. Houzvicka, I. Schmidt, A. Carlsson, *J. Am. Chem. Soc.* **2000**, *122*, 7116; c) K. Egeblad, C. H. Christensen, M. Kustova, C. H. Christensen, *Chem. Mater.* **2008**, *20*, 946; d) M. Choi, H. S. Cho, R. Srivastava, C. Venkatesan, D.-H. Choi, R. Ryoo, *Nat. Mater.* **2006**, *5*, 718.
[6] a) R. M. Dessau, E. W. Valyocsik, N. H. Goeke, *Zeolites* **1992**, *12*, 776; b) G. Lietz, K. H. Schnabel, Ch. Peuker, Th. Gross, W. Storek, J. Völter, *J. Catal.* **1994**, *148*, 562; c) D. Ohayon, R. L. V. Mao, D. Ciaravino, H. Hazel, A. Cochennec, N. Rolland, *Appl. Catal. A* **2001**, *217*, 241; d) J. C. Groen, L. A. A. Peffer, J. A. Moulijn, J. Perez-Ramirez, *Chem. Eur. J.* **2005**, *11*, 4983.
[7] a) M. Bjørgen, F. Joensen, M. S. Holm, U. Olsbye, K.-P. Lillerud, S. Svelle, *Appl. Catal. A* **2008**, *345*, 43; b) M. Ogura, S. Shinomiya, J. Tateno, M. Nomura, E. Kikuchi, M. Matsukata, *Appl. Catal. A* **2001**, *219*, 33.
[8] J. C. Groen, S. Abelló, L. A. Villaescusa, J. Pérez-Ramírez, *Microporous Mesoporous Mater.* **2008**, *114*, 93.
[9] X. Wei, P. G. Smirniotis, *Microporous Mesoporous Mater.* **2006**, *97*, 97.
[10] J. C. Groen, T. Sano, J. A. Moulijn, J. Pérez-Ramírez, *J. Catal.* **2007**, *251*, 21.
[11] R. L. V. Mao, A. Ramsaran, S. Xiao, J. Yao, V. Semmer, *J. Mater. Chem.* **1995**, *5*, 533.
[12] J. C. Groen, J. A. Moulijn, J. Pérez-Ramírez, *Ind. Eng. Chem. Res.* **2007**, *46*, 4193.
[13] J. C. Groen, J. C. Jansen, J. A. Moulijn, J. Pérez-Ramírez, *J. Phys. Chem. B* **2004**, *108*, 13062.
[14] J. C. Groen, J. A. Moulijn, J. Pérez-Ramírez, *Microporous Microporous Mater.* **2005**, *87*, 153.
[15] P. Prokesova-Fojtíková, S. Mintova, J. Cejka, N. Zilková, A. Zukal, *Microporous Microporous Mater.* **2006**, *92*, 154.
[16] M. S. Holm, S. Svelle, F. Joensen, P. Beato, C. H. Christensen, S. Bordiga, M. Bjørgen, *Appl. Catal. A*, **2008**, in press.
[17] C. Pazé, S. Bordiga, C. Lamberti, M. Salvalaggio, A. Zecchina, *J. Phys. Chem. B* **1997**, *101*, 4740.
[18] M. A. Camblor, A. Corma, S. Valencia, *J. Mater. Chem.* **1998**, *8*, 2137.

Received: December 9, 2008
Published Online: February 11, 2009

 © 2009 Wiley-VCH Verlag GmbH & Co. KGaA, Weinheim